Supplementary Material

Versatile interfacial modifier enabling efficient antimony selenosulfide indoor photovoltaics

Ming Wang[1, §], Weijia Zhao[1, §], Xin Yao[1, †], Zhirui Wang[1], Qi Gao[1], Hong Zhang[2, †], Fuling Guo[1], Yanqing Wang[1], Wangchao Chen[1, †]

[1]School of Chemistry and Chemical Engineering, Anhui Province Key Laboratory of Value-Added Catalytic Conversion and Reaction Engineering, Hefei University of Technology, Hefei 230009, China
[2]School of Mathematics and Physics Science and Engineering, Hebei University of Engineering, Handan 056038, China.

Materials

Chromium chloride ($CdCl_2$), thiourea (CH_4N_2S), thioacetamide (C_2H_5NS), sodium thiosulfate pentahydrate ($Na_2S_2O_3 \cdot 5H_2O$) and potassium antimony tartrate ($C_4H_4KO_7Sb \cdot 0.5H_2O$) were purchased from Sinopharm Chemical Reagent Co., Ltd. Selenourea (CH_4N_2Se) was purchased from TCI Development Co., Ltd. Fluorine tin oxide conductive glasses (FTO) and Tin oxide (SnO_2) colloidal dispersion liquid (12 wt% in H_2O) were obtained from Advanced Election Technology Co., Ltd. Petroleum ether (PE), chlorobenzene (CB), dichloromethane (DCM), *N*, *N*-dimethylformamide (DMF), ethyl acetate (EA), Lithium bis (trifluoromethylsulfhonyl) imide salt (Li-TFSI) and 4-tert-butylpyrdine (tBP) were purchased from Sigma-Aldrich. 2,2',7,7'-Tetrakis [*N*, *N*-di(4-methoxyphenyl)amino]-9,9'-spirobifluorene (Spiro-OMeTAD) was bought from Ying Kou Libra New Energy Technology Co., Ltd. All the above chemical reagents were used as received without extra purification, and the solvents were treated according to the standard procedures.

Synthesis

4,4'-(4,8-bis((2-ethylhexyl)oxy)benzo[1,2-*b*:4,5-*b*']dithiophene-2,6-diyl)bis(*N*,*N*-bis(4-methoxyp-henyl)aniline) (O-BDT)

The compound 1 (402.1 mg, 1 mmol) and compound 2 (905.8 mg, 2.1 mmol) were stirred together at 500 rpm in a mixed solution of toluene and THF (v:v, 1:1). The aqueous solution of K_2CO_3 (850 mg, 2 mL) and $Pd(PPh_3)_4$ (25 mg) were subsequently transferred to the aforementioned solution. Under the protection of N_2, the reflux reaction was stirred for 12 h at 100 °C. After cooling to R.T., the mixture was filtered and the residue was removed thoroughly. The crude product was purified by column chromatography employing the petroleum ether/dichloromethane (7:1, v/v) as eluent system. Finally, the product was collected as buff powder (747 mg, yield of 71%). ^{1}H NMR (600 MHz, $CDCl_3$) δ/ppm: 7.52 (t, *J* = 12.8 Hz, 6H), 7.09 (d, *J* = 8.8 Hz, 8H), 6.95 (d, *J* = 8.6 Hz, 4H), 6.86 (d, *J* = 8.9 Hz, 8H), 4.17 (s, 4H), 3.81 (s, 12H), 1.37 (s, 4H), 1.33 (s, 1H), 1.29 (s, 5H), 1.25 (s, 8H), 1.02 (t, *J* = 7.5 Hz, 6H), 0.93 (t, *J* = 7.0 Hz, 6H). ^{13}C NMR (151 MHz, $CDCl_3$)

δ/ppm: 156.10, 148.82, 143.26, 140.38, 132.53, 127.00, 126.82, 120.06, 114.72, 76.80, 55.49, 40.61, 30.43, 29.20, 23.84, 23.16, 14.20, 11.34.

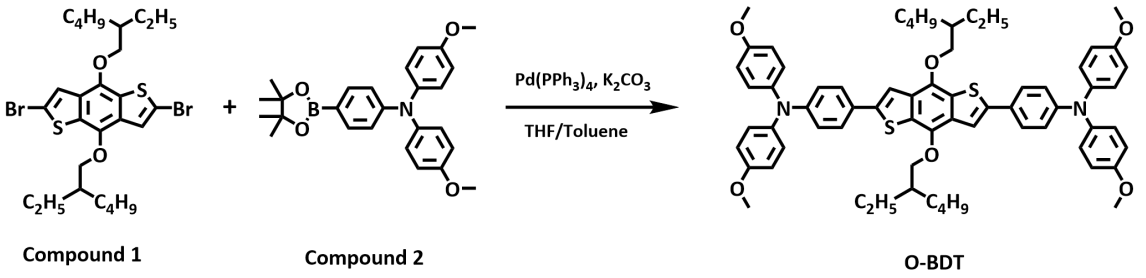

Scheme S1. Synthetic Route to O-BDT

Device fabrication

The FTO glass substrates were sequentially cleaned by ultrasonication in deionized water, ethanol and acetone for 30 min and dried with nitrogen flow. Then the substrates were treated in UV-ozone atmosphere for 30 min to improve the surface wetting. Composing of SnO_2 colloidal dispersion liquid and an aqueous solution in a volume ratio of 1:5, the SnO_2 solution was spin-coated on the substrates at a speed of 3000 rpm for 30 s, and then annealed at 150 °C for 30 min in air. The CdS layer was deposited on SnO_2 buried layer by chemical bath deposition. The $Sb_2(S,Se)_3$ film was fabricated through the hydrothermal method upon the CdS layer under 135 °C for 3 h. Subsequently, the sample was annealed for 10 min at 350 °C in a nitrogen atmosphere glovebox. The $C_4H_4KO_7Sb{\cdot}0.5H_2O$ (40 mM), $Na_2S_2O_3$ (140 mM) and CH_4N_2Se (3 mM) were used as Sb-source, S-source and Se-source in the precursor solution, respectively. The O-BDT solution dissolved in DMF (1 mg/mL) was spin-coated onto the $Sb_2(S,Se)_3$ film surface at 3000 rpm for 40 s, followed by annealing at 100 °C for 10 min. Subsequently, the HTM solution (36.6 mg Spiro-OMeTAD, 9.5 μL Co (III) TFSI and 14.5 μL tBP in 1 mL CB) was spin-coated on the substrates at 3000 rpm for 40 s, followed by annealing at 100 °C for 10 min. Finally, gold electrode (60 nm) was deposited by thermal evaporation on the HTL.

Characterization

Nuclear magnetic resonance (NMR) spectra were measured using the Bruker Advance III spectrometer. Ultraviolet-visible (UV-vis) absorption spectra was measured by the Thermo-Fisher Evolution 220. Cyclic voltammetry (CV) was conducted using the three-electrode system (glass carbon as working electrode, platinum wire as counter electrode

and Ag/AgCl as reference electrode) in dilute dichloromethane solution with 0.1 M tetrabutylammonium hexafluorophosphate (n-Bu_4NPF_6) as supporting electrolyte. The ferrocene/ferrocene$^+$ couple was employed as the external standard. X-ray photoelectron spectroscopy (XPS) was collected from the Thermo ESCALAB 250Xi with X-ray source of a monochromatic Al Kα (1486.6 eV) and the photoelectrons kinetic energy of 1 keV. Scanning electron microscopy (SEM) was collected on Regulus 8230 produced by Hitachi, where the electron beam accelerated at 5 kV. Atomic Force Microscope (AFM) and Kelvin Probe Force Microscopy (KPFM) images were obtained from the Bruker AXS Dimension Icon with Scan rate of 0.651 Hz and Scan Size of 1 μm. Current-Voltage (*I-V*) curves were registered by a solar simulator (Newport, 94083A) with a source meter (Keithley 2450) under 100 mW cm^{-2} illumination (AM 1.5G). The lux levels of LEDs (JHFL6060-W) were obtained by using a luxmeter (TES-1330A). The spectral irradiance of the indoor light source of 3312 K LED was measured with a high-precision fiber-optic spectrometer (Maya2000 Pro, Ocean Optics). Electrochemical impedance spectroscopy (EIS), Mott-Schottky and dark-state *J-V* diagrams were performed on Zennium Pro electrochemical workstation. Water contact angles were measured on Dataphysics OCA50Micro.

Calculation Details

Density functional theory (DFT) calculations were proceeded by CP2K code, using localized atomic DZVP-MOLOPT basis sets. The Perdew-Burke-Ernzerh (PBE) of functional was employed to describe the exchange-correlation interaction. The configuration of molecules at the interface was determined through Molecular Dynamics (MD) simulations. The MD simulations were performed at 300 K using the NVT ensemble, and the simulation time was about 4 ps with a time step of 1 fs. The trajectory was visualized by the VESTA package. $Sb_2(S,Se)_3$-terminated surface, got from the bulk structure of the Sb_2S_3 with Space group Pbnm. In the bulk structure relaxation, the Brillouin zone was sampled using a k-point mesh (2×6×2) centered at the Gamma point. The (130) surface of $Sb_2(S,Se)_3$ was the dominant surface for absorption layer. Here, the (130) surface of Sb_2S_3 was constructed firstly with a vacuum thickness of 20 Å added along the Z direction. Subsequently, we replaced S with Se in the (130) surface of Sb_2S_3 to construct the (130) surface of $Sb_2(S,Se)_3$. The electrostatic potential (ESP) analysis for the O-BDT

molecule was performed with B3LYP functional using Dmol3. To simplify the computation, the long alkyl side chains were replaced by methyl. Then, Vienna Ab Initio Simulation Package (VASP) program was used to investigate the adsorption energy between the O-BDT based molecules and $Sb_2(S,Se)_3$.

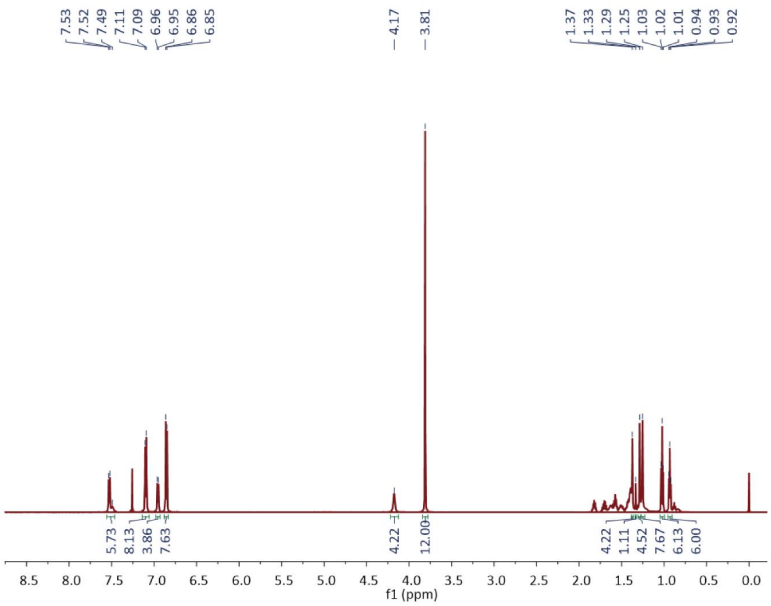

Fig. S1. ^{1}H NMR spectrum of O-BDT.

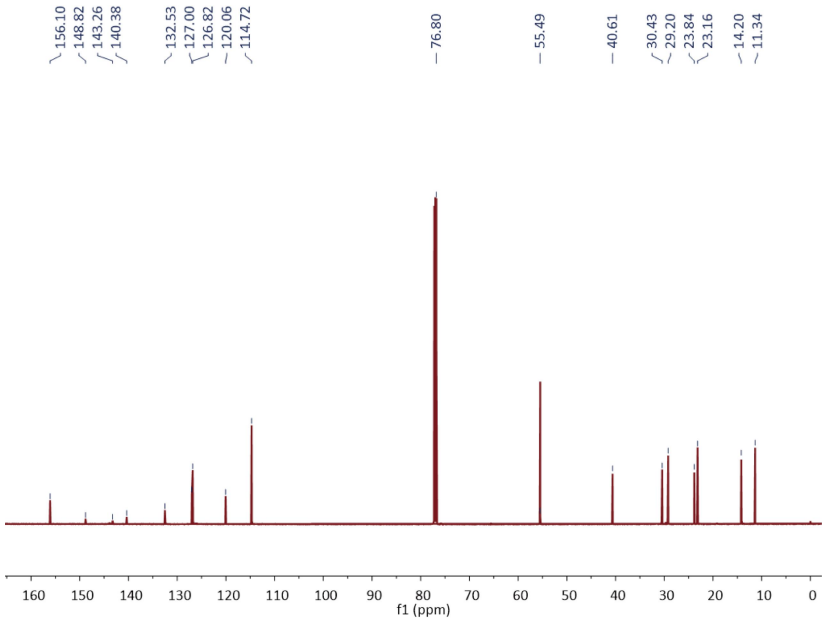

Fig. S2. ^{13}C NMR spectrum of O-BDT.

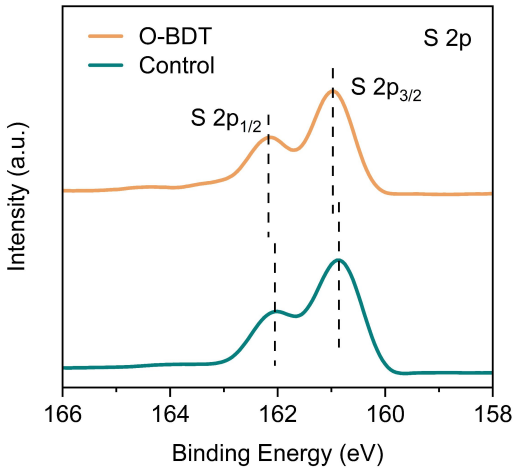

Fig. S3. S 2*p* XPS spectra of the control and O-BDT treated $Sb_2(S,Se)_3$ films.

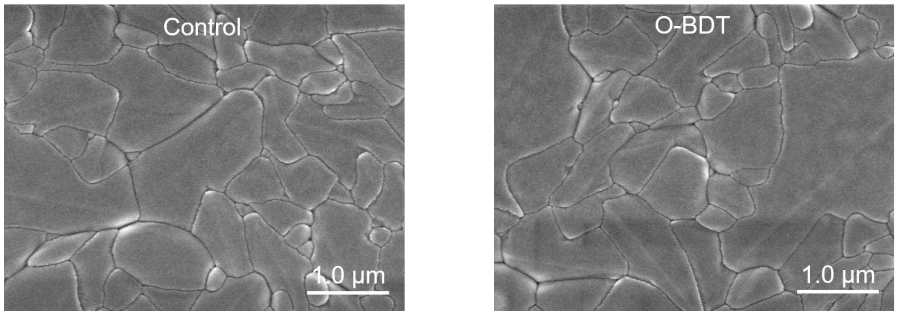

Fig. S4. Surface morphologies of the control and O-BDT-treated $Sb_2(S,Se)_3$ films.

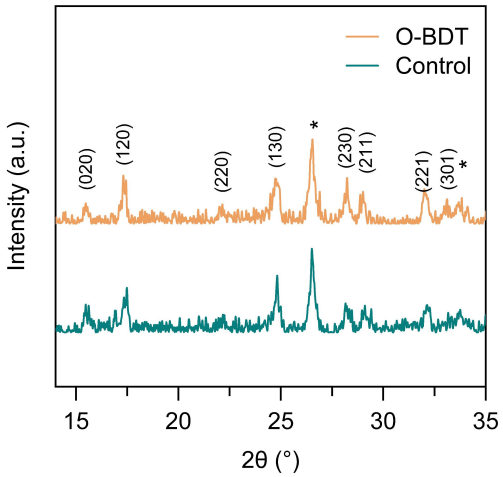

Fig. S5. XRD spectra of the control and O-BDT-treated $Sb_2(S,Se)_3$ films.

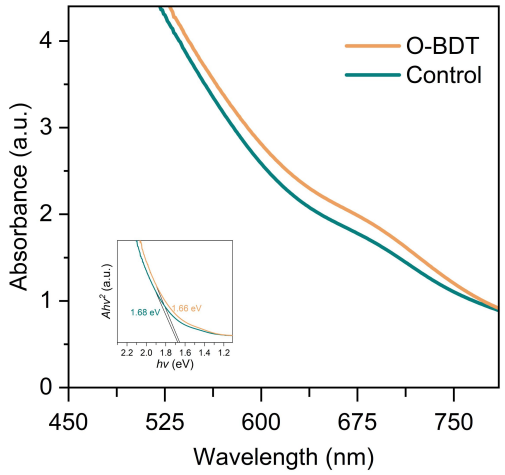

Fig. S6. UV-vis absorption spectra and corresponding Tauc plots of the control and O-BDT-treated $Sb_2(S,Se)_3$ films.

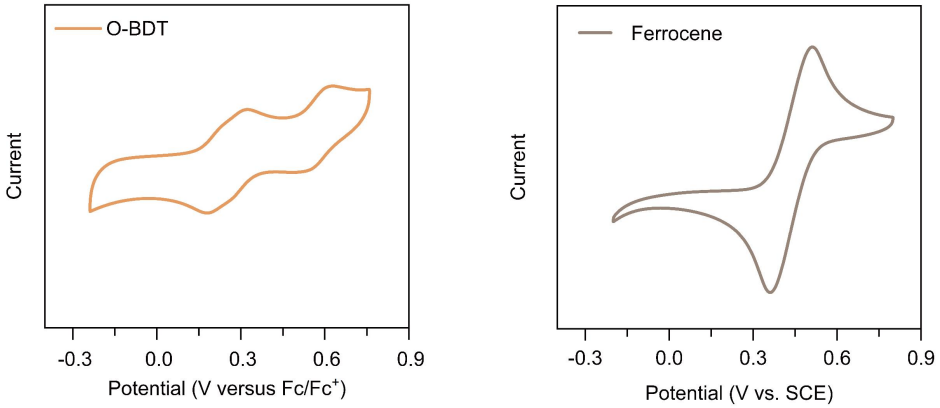

Fig. S7. CV curve of O-BDT and Fc/Fc^+.

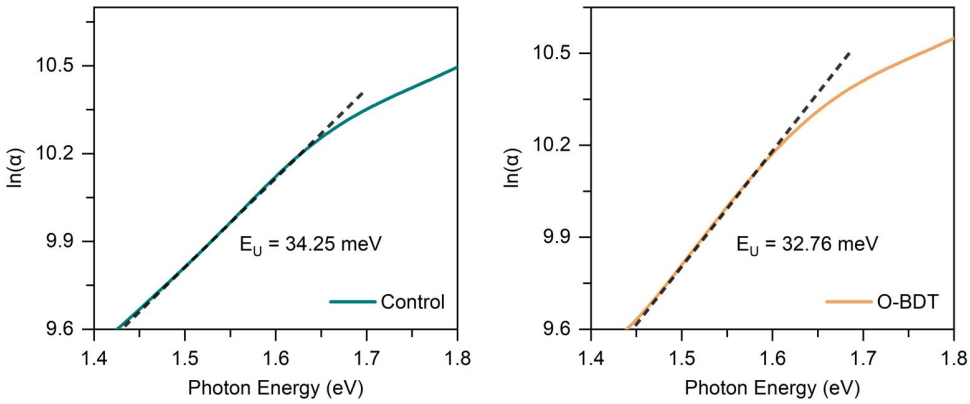

Fig. S8. Urbach Energy (E_U) of the control and O-BDT-treated $Sb_2(S,Se)_3$ films.

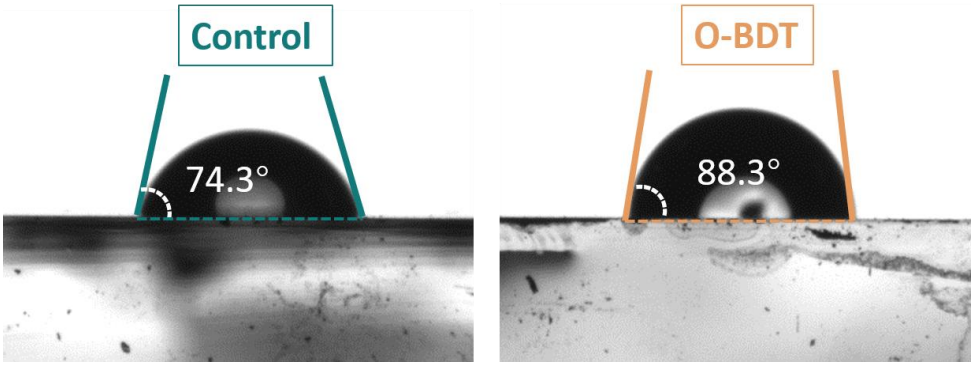

Fig. S9. Water contact angles of the control and O-BDT-treated $Sb_2(S,Se)_3$ films.

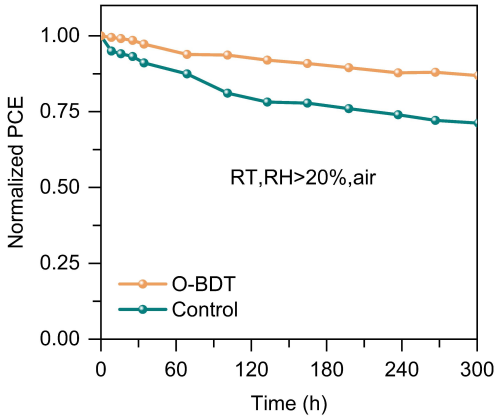

Figure S10. Normalization PCE curves of the control and O-BDT-treated $Sb_2(S,Se)_3$ devices at the beginning and after storage in ambient air for 300 h.

Table S1. Photovoltaic parameters of the $Sb_2(S,Se)_3$ devices based on O-BDT with different concentrations.

Concentration (mg/mL)	V_{OC} (V)	J_{SC} (mA cm^{-2})	FF (%)	PCE (%)
0	0.705	17.55	60.21	7.45
0.5	0.709	17.76	60.57	7.63
0.8	0.713	18.03	61.11	7.86
1.0	0.718	18.20	61.30	8.01
1.2	0.711	17.97	61.02	7.80